

Prototyping of Microfluidic Devices in Poly(dimethylsiloxane) Using Solid-Object Printing

J. Cooper McDonald, Michael L. Chabiny, Steven J. Metallo, Janelle R. Anderson, Abraham D. Stroock, and George M. Whitesides*

Department of Chemistry and Chemical Biology, Harvard University, 12 Oxford Street, Cambridge, Massachusetts 02138

A solid-object printer was used to produce masters for the fabrication of microfluidic devices in poly(dimethylsiloxane) (PDMS). The printer provides an alternative to photolithography for applications where features of >250 μm are needed. Solid-object printing is capable of delivering objects that have dimensions as large as $250 \times 190 \times 200$ mm (x, y, z) with feature sizes that can range from 10 cm to $250 \mu\text{m}$. The user designs a device in 3-D in a CAD program, and the CAD file is used by the printer to fabricate a master directly without the need for a mask. The printer can produce complex structures, including multilevel features, in one unattended printing. The masters are robust and inexpensive and can be fabricated rapidly. Once a master was obtained, a PDMS replica was fabricated by molding against it and used to fabricate a microfluidic device. The capabilities of this method are demonstrated by fabricating devices that contain multilevel and tall features, devices that cover a large area ($\sim 150 \text{ cm}^2$), and devices that contain nonintersecting, crossing channels.

Solid-object printers are a relatively new tool for the production of prototype 3-D structures.¹ The printers operate either by printing a thermoplastic polymer that solidifies after extrusion or by printing a binding material that joins regions of a predeposited layer of powder together. In this work, we use a solid-object printer that produces structures in a thermoplastic organic material against which we mold poly(dimethylsiloxane) (PDMS). These molded structures are used to prototype microfluidic devices.

Microfluidic devices have been described for many applications.^{2–6} One of the most important of these is bioanalysis: e.g., capillary electrophoresis, chromatography, PCR, and nucleic acid sequencing.^{7–18} Many applications of microfluidic devices are compatible with, or require, large channels ($>200 \mu\text{m}$), and it must

be possible to connect them easily to the outside world. In addition, microfluidic devices have broader capability if they can be designed to incorporate 3-D and multilevel channel structures; an example is a cooling coil around a central channel.¹⁹

Rapid prototyping of microfluidic devices is important in a research setting where it is necessary to complete multiple cycles of design, fabrication, and testing in a short period of time.^{5,20} Fabrication in silicon or glass, two common materials used for microfluidics, requires chemical etching or more complex techniques such as reactive ion etching (RIE) and fusion bonding.^{21,22} All of these processes may be difficult if facilities are not available. Polymers are attractive materials for rapid prototyping, since they can be inexpensive, mechanically robust, disposable, optically transparent, and gas permeable, and the properties of their surfaces can often be modified chemically. The fabrication of microfluidic devices in polymers typically involves casting, injection molding, or hot embossing.^{4,23} Much of our work in polymeric microfluidics has focused on using photolithography to produce “masters” consisting of a positive bas-relief structure of photoresist

* To whom correspondence should be addressed: (telephone) (617) 495–9430; (telefax) (617) 495–9857; (e-mail) gwhitesides@gmwgroup.harvard.edu.

(1) Carrion, A. *Rapid Prototyping J.* **1997**, *3*, 99–115.
(2) Kovacs, G. T. A. *Micromachined Transducers Sourcebook*; McGraw-Hill: New York, 1998.
(3) van den Berg, A.; Bergveld, P., Eds. *Micro Total Analysis Systems*; Kluwer: Boston, 1995.
(4) Becker, H.; Gartner, C. *Electrophoresis* **2000**, *21*, 12–26.
(5) McDonald, J. C.; Duffy, D. C.; Anderson, J. R.; Chiu, D. T.; Wu, H.; Schueller, O. J. A.; Whitesides, G. M. *Electrophoresis* **2000**, *21*, 27–40.
(6) Bruin, G. J. M. *Electrophoresis* **2000**, *21*, 3931–3951.
(7) Effenhauser, C. S.; Bruin, G. J. M.; Paulus, A.; Ehrat, M. *Anal. Chem.* **1997**, *69*, 3451–3457.

(8) Duffy, D. C.; Gillis, H. L.; Lin, J.; Sheppard, N. F.; Kellogg, G. J. *Anal. Chem.* **1999**, *71*, 4669–4678.
(9) Bernard, A.; Michel, B.; Delamar, E. *Anal. Chem.* **2001**, *73*, 8–12.
(10) Fu, A. Y.; Spence, C.; Scherer, A.; Arnold, F. H.; Quake, S. R. *Nat. Biotechnol.* **1999**, *17*, 1109–1111.
(11) Harrison, D. J.; Fluri, K.; Seiler, K.; Fan, Z.; Effenhauser, C. S.; Manz, A. *Science* **1993**, *261*, 895–897.
(12) Kutter, J. P.; Jacobson, S. C.; Matsubara, N.; Ramsey, J. M. *Anal. Chem.* **1998**, *70*, 3291–3297.
(13) Northrup, M. A.; Bennett, B.; Hadley, D.; Landre, P. L.; Lehew, S.; Richards, J.; Stratton, P. *Anal. Chem.* **1998**, *70*, 918–922.
(14) Simpson, P. C.; Roach, D.; Woolley, A. T.; Thorsen, T.; Johnston, R.; Sensabaugh, G. F.; Mathies, R. A. *Proc. Natl. Acad. Sci. U.S.A.* **1998**, *95*, 2256–2261.
(15) Takayama, S.; McDonald, J. C.; Ostuni, E.; Liang, M. N.; Kenis, P. J. A.; Ismagilov, R. F.; Whitesides, G. M. *Proc. Natl. Acad. Sci. U.S.A.* **1999**, *96*, 5545–5548.
(16) Vahey, P. G.; Park, S. H.; Marquardt, B. J.; Xia, Y.; Burgess, L. W.; Synovec, R. E. *Talanta* **2000**, *51*, 1205–1212.
(17) Woolley, A. T.; Mathies, R. A. *Anal. Chem.* **1995**, *67*, 3676–3680.
(18) Burns, M. A.; Johnson, B. N.; Brahmasandra, S. N.; Handique, K.; Webster, J. R.; Krishnan, M.; Sammarco, T. S.; Man, P. M.; Jones, D.; Heldinger, D.; Mastrangelo, C. H.; Burke, D. T. *Science* **1998**, *282*, 484–487.
(19) Anderson, J. R.; Chiu, D. T.; Jackman, R. J.; Cherniavskaya, O.; McDonald, J. C.; Wu, H.; Whitesides, S. H.; Whitesides, G. M. *Anal. Chem.* **2000**, *72*, 3158–3164.
(20) Duffy, D. C.; McDonald, J. C.; Schueller, O. J. A.; Whitesides, G. M. *Anal. Chem.* **1998**, *70*, 4974–4984.
(21) Madou, M. *Fundamentals of Microfabrication*; CRC: New York, 1997.
(22) Maluf, N. *An Introduction to Microelectromechanical Systems Engineering*; Artech: Boston, 2000.
(23) Soper, S. A.; Ford, S. M.; Qi, S.; McCarter, R. L.; Kelly, K.; Murphy, M. C. *Anal. Chem.* **2000**, *72*, 642A–651A.

on a Si wafer for molding polymers such as PDMS. We previously developed a method for rapidly prototyping microfluidic devices using contact photolithography by replacing the chrome mask that is normally used with a transparency printed with a high-resolution printer; this technique is now widely used.^{5,8,16,19,20,24–28} With this technique, one can produce devices with feature sizes of $>20\ \mu\text{m}$ at low cost in 24 h.

In many cases, fabrication of the master limits the complexity and size of the devices that can be made. A major limitation of photolithography is that it is an inherently 2-D technique. This characteristic makes it difficult to fabricate masters with curved surfaces, tall features ($>1\ \text{mm}$), or features requiring more than one level of fabrication. It is also difficult to make large-area, multilevel structures, since the size of the mask aligner and Si wafers used in photolithography determines the maximum area of devices produced; typical sizes for academic users are 3–4 in. in their largest dimension. Three-dimensional photolithography—stereolithography—is available, but this methodology is more expensive and time-consuming than 2-D photolithography.^{21,23,29}

In contrast to photolithography, solid-object printing can produce objects having dimensions up to several inches in x , y , and z . More importantly, the printers can make multilevel structures, curved surfaces, and true 3-D models quickly. Unlike photolithography, once an object is defined in a CAD file, there is no need for multiple masks and exposures. Solid-object printers are less expensive (\$50 000) than mask aligners ($>$ \$200 000) and readily available for use. Applications of solid-object printing include prototyping design models, producing molds for casting metals and ceramics, and fabricating supports for bio/tissue engineering.^{30–32} Currently available commercial instruments, however, generate structures with poorer resolution (features of $>250\ \mu\text{m}$) and greater surface roughness ($\sim 8\ \mu\text{m}$) than does photolithography.

We demonstrate the ability of solid-object printing to produce masters for the fabrication of microfluidic devices that contain multilevel structures and 3-D channels and ones that mate a standard multichannel pipettor with microfluidic channels.

RESULTS AND DISCUSSION

A. Fabrication of Devices. Microfluidic devices were fabricated from masters produced by solid-object printing (Figure 1). The design for the mold was defined in 3-D in a CAD program. The solid-object printer then divided the file into horizontal sections and printed the mold layer by layer. The mold produced had surface roughness caused by the resolution of the printer

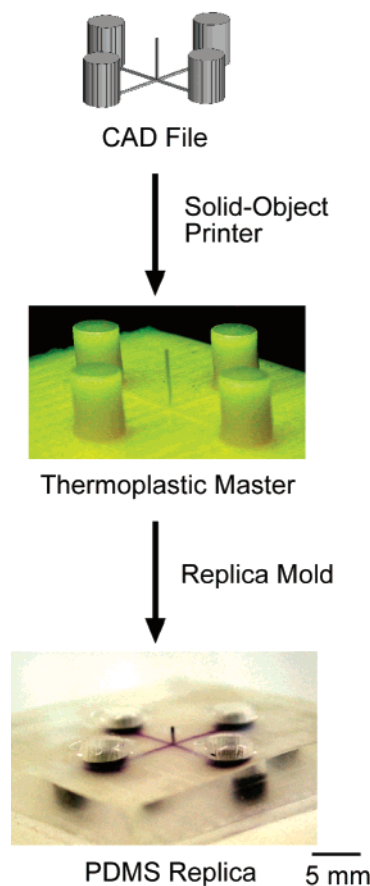


Figure 1. Scheme for prototyping devices in PDMS using solid-object printing. First, a CAD file is generated that defines the system in 3-D. Next, the software controlling the solid-object printer divides that file into many layers. A print head prints the object layer by layer ($300 \times 400 \times 600\ \text{dpi}$ in x , y , and z , respectively). The ink is a melted thermoplastic material that cools and solidifies once it leaves the print head. Once the object is printed, liquid PDMS prepolymer is poured over the mold and cured at $70\ ^\circ\text{C}$ for 1.5 h. The PDMS replica is then peeled from the thermoplastic mold. The device depicted in this figure is a 3-D cross of microfluidic channels conformally sealed to a flat piece of PDMS and filled with ink: two channels intersect in the x , y plane, and a third channel comes out of the plane at the intersection. The channels had square cross sections ($500 \times 500\ \mu\text{m}^2$). The cylinders define fluid reservoirs and are 4 mm in diameter and 5 mm tall.

($300 \times 400 \times 600\ \text{dpi}$, $85 \times 64 \times 42\ \mu\text{m}^3$ for x , y , and z , respectively). The build time is $\sim 2\ \text{h}$ for an object having dimensions of $12 \times 12 \times 1\ \text{cm}^3$. The thermoplastic build material (Thermojet 2000) used to make the mold is a proprietary mixture of hydrocarbons, amides, urethanes, and esters. It has a melting point of ~ 80 – $90\ ^\circ\text{C}$, and it is incompatible with organic solvents. The solvents dissolve a component of the build material, and when these solvents evaporate, the stress causes the build material to crack. The solid-object printer reduced the number of steps in fabrication of masters, compared to the corresponding process based on photolithography. For example, a three-level structure requires three different masks, careful alignment, and three exposures in photolithography; in solid-object printing, the CAD file is printed directly, in one step, to produce the final object. A thick base ($\sim 6\ \text{mm}$) is necessary on the molds to facilitate removal of the mold from the printer.

- (24) Martin, R. S.; Gawron, A. J.; Lunte, S. M.; Henry, C. S. *Anal. Chem.* **2000**, *72*, 3196–3202.
- (25) Kim, J.-S.; Knapp, D. R. *J. Am. Soc. Mass. Spectrom.* **2001**, *12*, 463–469.
- (26) Hong, J. W.; Fujii, T.; Seki, M.; Yamamoto, T.; Endo, I. *Electrophoresis* **2001**, *22*, 328–333.
- (27) Liu, Y.; Fanguy, J. C.; Bledsoe, J. M.; Henry, C. S. *Anal. Chem.* **2000**, *72*, 5939–5944.
- (28) Eteshola, E.; Leckband, D. *Sens. Actuators, B* **2001**, *72*, 129–133.
- (29) Ikuta, K.; Hirowatari, K.; Ogata, T. *IEEE MEMS* **1994**, 1–6.
- (30) Uhland, S. A.; Holman, R. K.; Cima, M. J.; Sachs, E.; Enokido, Y. In *Solid Freeform and Additive Fabrication*; Dimos, D., Danforth, S. C., Cima, M. J., Eds.; MRS: Warrendale, PA, 1999; pp 153–158.
- (31) Cima, M. J.; Sachs, E.; Cima, L. G.; Yoo, J.; Khanuja, S.; Borland, S. W.; Wu, B.; Giordano, R. A. *Solid Freeform Fabr. Symp. Proc.* 1994; pp 181–190.
- (32) Katstra, W. E.; Palazzolo, R. D.; Rowe, C. W.; Giritioglu, B.; Teung, P.; Cima, M. J. *J. Controlled Release* **2000**, *66*, 1–9.

After generating the master using solid-object printing, we poured liquid PDMS prepolymer over the mold and cured it for 1.5 h at 70 °C. The PDMS replica was then peeled from the thermoplastic mold: PDMS did not adhere to the mold. Because the master was a thermoplastic material, it could be damaged by deformation, especially just after removal from the oven. Allowing the thermoplastic to cool to room temperature before handling reduced this problem. We have cast replicas from molds repeatedly (more than 10 replicas) with careful handling. Figure 2 shows scanning electron micrographs of PDMS replicas. The PDMS replicated the surface roughness of the thermoplastic mold. We measured the surface roughness to have a maximum deviation of $\pm \sim 9 \mu\text{m}$ by profilometry.

We have developed two methods of sealing devices fabricated in PDMS.⁵ Devices can be sealed reversibly or irreversibly. Simple conformal contact to a flat surface provides an adequate seal for low-pressure flows (<5 psi). Exposing a PDMS replica and another flat surface, e.g., PDMS, glass, or Si, to an air plasma for 1 min and then bringing the surfaces into contact causes a strong bond to form, and the channels are rendered hydrophilic. The surface roughness present in PDMS replicas of masters produced by solid-object printing complicated sealing compared to sealing replicas of masters produced by photolithography. In this work, we could seal PDMS reversibly and irreversibly by applying pressure to force the replica to conform to a flat surface. By applying pressure for a short duration (<30 s), we could seal devices reversibly to PDMS and also to cellophane or silicone tape and irreversibly to PDMS and glass. Reversible sealing to rigid surfaces such as glass was not possible without continuously applied pressure.

It was possible to smooth the surface of the masters by melting and annealing the thermoplastic material against a transparency. We fabricated “inverse” masters in which the channels were in negative relief in the structure. The master was then placed in contact with a transparency and heated at 95 °C for 5 min on a hot plate. The thermoplastic melted into contact with the transparency. The annealed, smoothed master detached from the transparency after being placed in a freezer at $-20 \text{ }^\circ\text{C}$ for 30 min. A transparency was used because it was flexible and easily detached from the thermoplastic. PDMS was then molded against the annealed master to produce a PDMS master having channels in positive relief. The PDMS master was silanized and used to produce replicas with embedded channels. The surface of one of these annealed PDMS replicas was much smoother than one molded directly against a thermoplastic master that had not been annealed, and it could be sealed reversibly or irreversibly to rigid materials (Figure 2).

B. Microfluidic Devices. We have fabricated a number of microfluidic devices that demonstrate the abilities of solid-object printing. Two of the devices emphasized multilevel features, one exploited the ability of the printer to produce large (centimeter) and small (submillimeter) features in the same device to facilitate connections between the laboratory (macroscopic) and channels (microscopic), and one demonstrated the fabrication of 3-D systems of channels.

3-D Cross. Many microfluidic applications require multilevel features: for example, the ability to incorporate vertical channels allows for vias between two levels of channels and for insertion of capillaries or fiber optics at specific locations within channels.

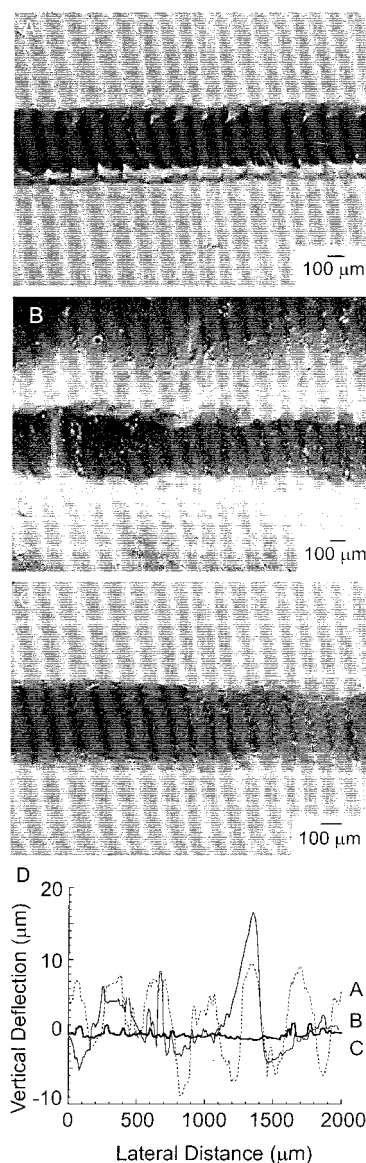


Figure 2. Scanning electron micrographs of PDMS replicas of the thermoplastic mold. (A) This micrograph shows a 500- μm channel molded against a thermoplastic master that contained features in positive relief. The micrograph shows the surface roughness present in the mold. (B) This image shows a 500- μm channel molded using an unannealed master with features in negative relief. The surface roughness is reduced in comparison to the master with positive relief for reasons unknown to the manufacturer of the printer. The master was replicated in PDMS; this replica, with features in positive relief, then served as a master for molding of PDMS with embedded channels. (C) This micrograph shows a 500- μm channel molded using an annealed master that contained features in negative relief. An inverse master containing features in negative relief was placed against a transparency and heated to 95 °C on a hot plate. After 5 min, the master and transparency were placed in a freezer ($-20 \text{ }^\circ\text{C}$) until the transparency detached from the surface of the master. The PDMS replica with embedded channels was fabricated as in (B). (D) Profilometry of surface roughness of channels molded from positive relief masters (dashed line), negative relief masters (thin, solid line), and annealed negative relief masters (thick, solid line). A periodic pattern of grooves and ridges ($\sim 10\text{--}20 \mu\text{m}$ from trough to crest) was present in the positive sample. A pattern of grooves and ridges was also present in the unannealed sample, but the frequency of the grooves was lower than in the positive sample. No pattern of grooves was present in the annealed sample. Profilometry was performed on epoxy replicas of the molds (see Experimental Section).

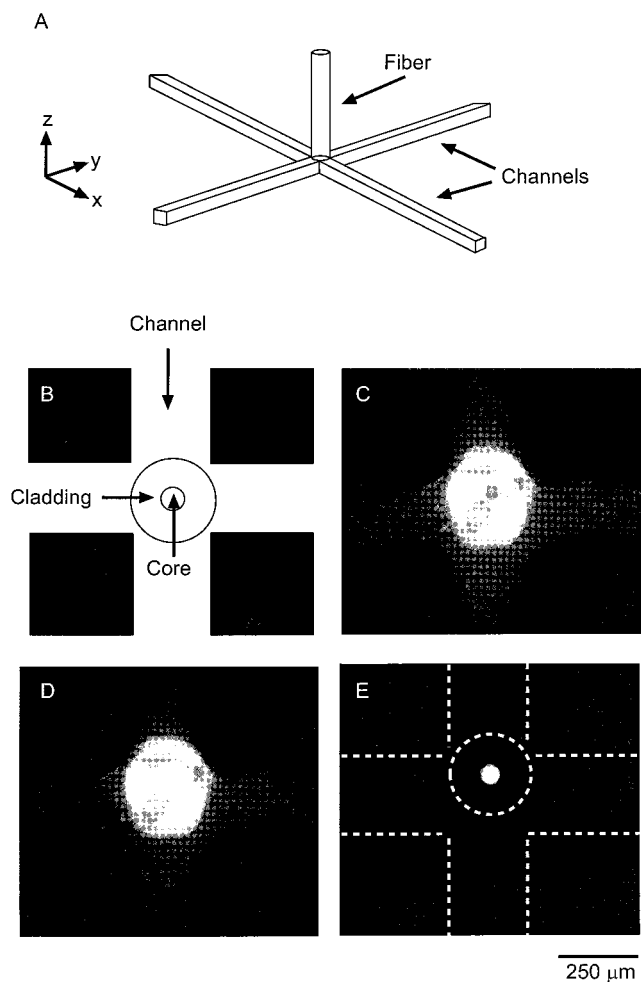


Figure 3. Optical coupling of an optical fiber to the center of a 3-D cross. (A) Two horizontal channels ($250\ \mu\text{m}$ wide, $250\ \mu\text{m}$ tall) intersect at right angles in the x, y plane; at this intersection, a square vertical channel ($250\ \mu\text{m}$ wide, $3\ \text{mm}$ tall) is also present. An optical fiber is inserted into the vertical channel and aligned at the intersection of the horizontal channels. (B) Schematic bottom view of the device showing the crossing channels and the cladding ($125\ \mu\text{m}$ thick) and core ($50\ \mu\text{m}$ in diameter) of the fiber. (C–E) Fluorescent micrographs of the channel system filled with a solution of fluorescein. (C) Channel system illuminated with blue light from the microscope. (D) Channel system illuminated with blue light from the microscope and with light from a blue LED coupled into the fiber. (E) Channel system with only light coupled into the fiber. Dashed lines indicate the approximate locations of the channels and cladding. The fiber is slightly misaligned from the intersection of the channels. Torque from bending the fiber to align the fiber with the source of illumination caused this misalignment.

Figure 1 shows a 3-D microfluidic cross comprising two horizontal channels oriented 90° from one another and a vertical channel that was $5\ \text{mm}$ tall. Vertical features of this height are difficult to fabricate using conventional lithography. The same master, produced using photolithography, would require multiple cycles of spin coating, alignment, and exposure. The solid-object printer produced the finished master in a single round of printing.

Fiber-optic sensors³³ have been developed for analysis of solutions, and the fabrication of a 3-D cross allows an optical fiber

to be inserted vertically into a channel system at a precise location. The 3-D channel also allows the fiber to be removed and replaced if necessary. Figure 3 shows an optical fiber inserted into a 3-mm-tall vertical channel. The vertical channel aligned the fiber with the intersection of the two horizontal channels. The walls of the PDMS channel conformed to the fiber, and fluid could not flow into the vertical channel.

When the PDMS was removed from the mold, the narrow post of thermoplastic material that forms the vertical channel detached from the master and remained in the PDMS replica. We removed this material from the PDMS replica using a heat gun to melt the material and suction to remove it from the channel. Although the mold was destroyed in this case, we could replicate the mold in a harder material (e.g., epoxy) from the PDMS replica (see Experimental Section). The ability to remove material from the mold trapped inside a PDMS replica allows for the design of at least simple sacrificial molds—i.e., molds that are destroyed in the process of fabricating a device.³⁴

Mixer for Flows at Low Reynolds Number. Another application of multilevel devices is that of a recently developed microfluidic mixer (Figure 4).³⁵ Mixing in low Reynolds number (Re) flows (typical of microfluidic flows or polymer processing) is difficult because flow is laminar, and any mixing occurs only by diffusion transverse to the flow. This diffusive motion across the channel is typically slow compared to the movement of fluid with the flow. To decrease the time for mixing in microfluidic channels, a mixer must, in effect, be able to shorten the time necessary for diffusion to mix the solutions completely. The mixer reported here comprised one large channel with smaller, chevron-shaped indentations on one wall. Chevrons were grouped in sets of 6 with a total of 20 sets present in the device. The chevrons were not centered in the channel (Figure 4A): the vertexes of the chevrons were located $0.7\ \text{mm}$ from one sidewall and $1.3\ \text{mm}$ from the other. The sidewall that the vertexes of the chevrons were closer to alternated from set to set. The diagonally oriented grooves that make up the branches of the chevrons generate a transverse component of flow near the structured surface when fluid is pressure pumped through the channel. The transverse flow forces fluid to recirculate and generate a cellular flow over each branch of the chevron; the width of the cell is the same as the width of the branch of the chevron pattern (Figure 4C). Alternating the orientation of the chevrons produces a chaotic flow (the paths of adjacent volumes diverge exponentially with distance traveled down the channel).³⁶ The distance that diffusion must act to mix also drops exponentially with distance along the channel.³⁵ A channel without the chevrons does not allow transverse flows; diffusional mixing requires a longer time than in a channel with chevrons. The mold for this device had walls around its perimeter that contained the liquid PDMS during curing and defined the overall shape of the PDMS replica, as well as the position of the channel system relative to the edges.

Figure 5 shows a comparison between a mixer and a similar channel without the chevrons (nonmixer). In this example, two

(34) Dharmatilleke, S.; Henderson, H. T. *Microelectromech. Syst.* **2000**, *2*, 413–418.

(35) Stroock, A. D.; Dertinger, S. K. W.; Adjari, A.; Mezić, I.; Stone, H. A.; Whitesides, G. M. *Science* **2002**, *295*, 647–651.

(36) Ottino, J. M. *The Kinematics of Mixing: Stretching, Chaos, and Transport*; Cambridge University Press: Cambridge, U.K., 1989.

(33) Ferguson, J. A.; Steemers, F. J.; Walt, D. R. *Anal. Chem.* **2000**, *72*, 5618–5624.

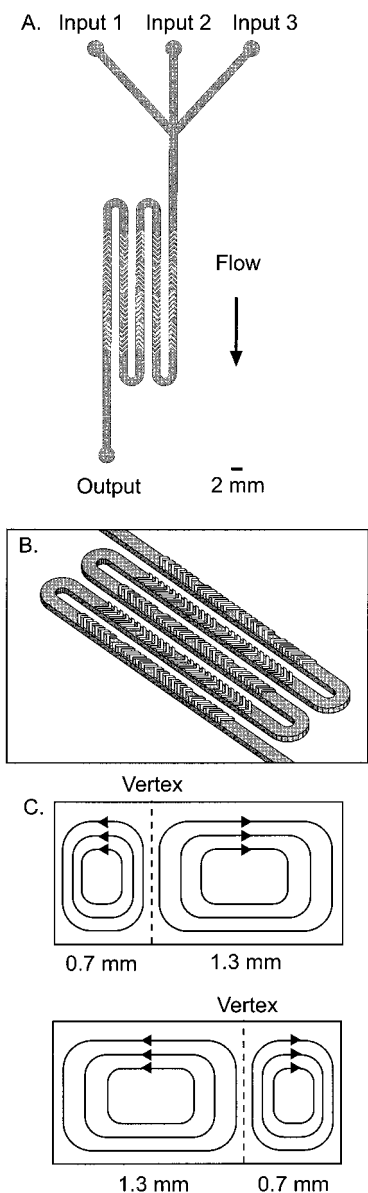


Figure 4. Design of a CAD file for a mold to produce a fluidic mixer. (A) Top view of the channel. The main channel (light gray) is 2 mm wide and 1 mm tall. The top wall of this channel contains 20 sets of 6 chevrons (white) ($400\ \mu\text{m}$ wide and $400\ \mu\text{m}$ tall). The channel is designed to mix up to three laminar flows from the inputs. (B) Closeup view of the chevrons. (C) Schematic view of cellular flow in the channel. Two cells are present that correspond to the widths of the branches of the chevrons. The alternating pattern of the chevrons causes an alternating pattern of cellular flow.

laminar flows of liquids, 20% water–80% glycerol with and without purple ink, flowed through the devices. The water–glycerol solution was used in order to ensure a low Re ($Re \sim 0.06$). At the flow speed used, broadening by diffusion was minimal ($\sim 50\ \mu\text{m}$ over the length of the channel). Mixing also occurred in aqueous solutions without glycerol ($Re > 5$), but we wished to demonstrate the mixer at low Re since low Re provides a more stringent test for mixing. In addition, commercial samples of some enzymes (e.g., ligase) contain glycerol, and the mixer could dilute these samples on chip with aqueous solutions. The mixer produced a nearly uniform intensity across the channel, and the nonmixer showed very little mixing.

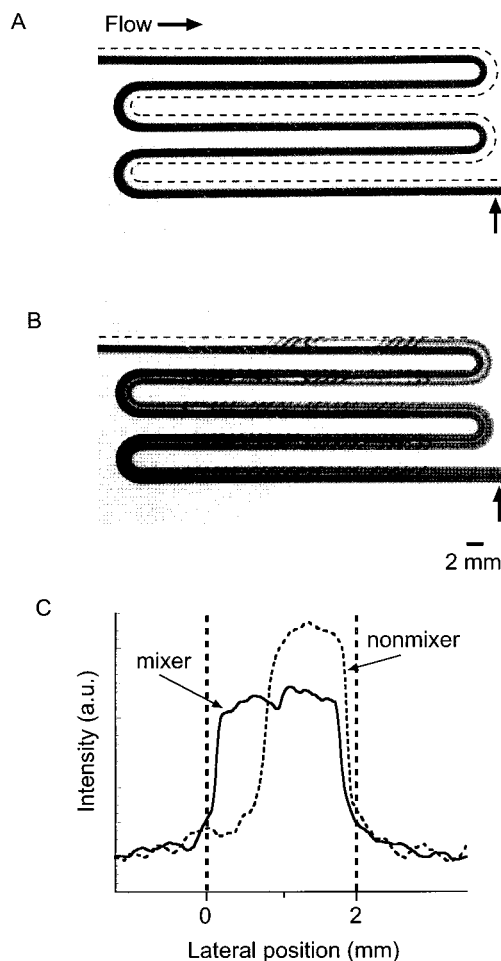


Figure 5. Mixing in a large-area microfluidic device. Inputs 1 and 3 from Figure 4 were used for these data. (A) Optical micrograph of a “nonmixer” (channel without chevrons) containing two laminar flows, 20% water–80% glycerol and water–glycerol containing purple ink. (B) Optical micrograph of a mixer containing two laminar flows that are mixed by the creation of transverse flows in the channel.³⁵ The fluids for both the mixer and nonmixer were pumped at 15 mL/h. Dashed lines indicate the boundaries of the channel. (C) Graph of intensity versus lateral position taken at the end of the channels (arrows in A and B). For the nonmixer (dashed line), the intensity is confined to approximately half of the channel. For the mixer (solid line), a more uniform intensity is seen across the channel indicating more efficient mixing. The integrated areas of the intensity curves were normalized to one another.

Interface between a Pipettor and Microfluidic Channels.

Connections between microfluidic channels and the external world require features that span dimensions from micrometers to centimeters. We exploited the fact that the solid-object printer can produce features in this range to fabricate a device that enables a user to address many microfluidic channels simultaneously using commonly available laboratory equipment. Figure 6 shows a scheme for mating a 12-channel pipettor, commonly used with 96-well plates, to microfluidic channels. The device covered an area larger ($13 \times 12\ \text{cm}^2$) than a standard 3-in. Si wafer and contained raised cylinders that formed well-defined reservoirs for fluids. The microfluidic channels were arranged such that they were parallel in the middle of the device so that they could all be observed simultaneously. The channel system was sealed with two pieces of silicone tape (Figure 6A). The two pieces of tape

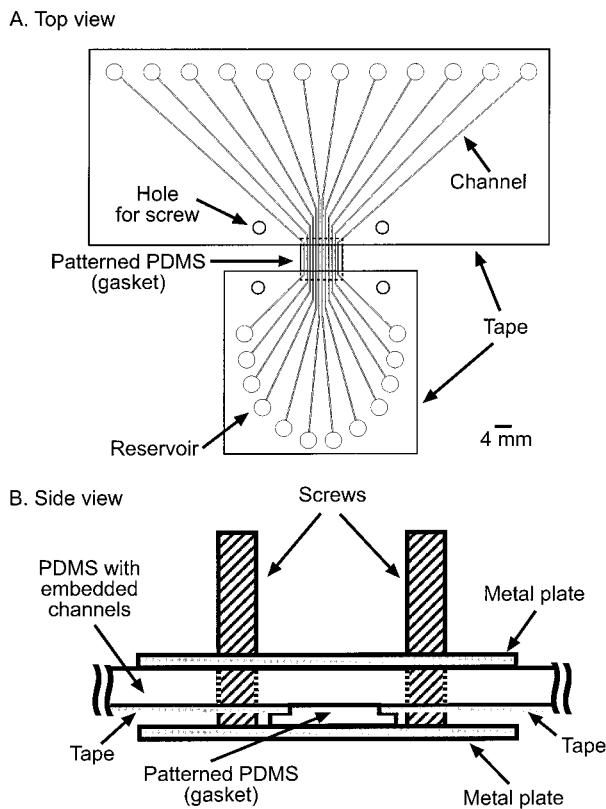


Figure 6. Scheme for a device to mate a 12-channel pipettor with microfluidic channels. (A) Twelve input reservoirs (3-mm diameter and 2 mm tall) were molded to match a standard 12-channel pipettor (9 mm apart). Each of these reservoirs is connected to a microfluidic channel (250 μm wide and 250 μm tall). The 12 output reservoirs are positioned in order to make each channel the same length. In the middle of the device, the 12 channels are parallel and spaced apart by 500 μm . The PDMS replica was sealed with two pieces of silicone tape, except for the central region where the channels are parallel. Four holes for screws are present in order for the device to be mounted in a clamp. A small piece of PDMS (1 \times 1 cm^2 , \sim 1 mm thick) was placed in contact with the exposed region of the channel to provide a surface for the patterned adsorption of proteins and overlapped the silicone tape (dashed lines) to provide a watertight seal. (B) Four screws attached to a metal plate were inserted into the PDMS with embedded channels. A second metal plate was then added, and the two PDMS pieces were clamped together between the metal plates by using wing nuts to apply pressure. The applied pressure caused the small piece of PDMS to deform around the edges of the silicone tape and created a tight seal with the larger piece of PDMS.

were arranged such that the region of the device with the channels in parallel was left unsealed. Four holes for screws were cut out of the PDMS and tape. We placed a small piece of PDMS (\sim 1 \times 1 cm^2 , \sim 1 mm thick) against the open channels; this piece overlapped the silicone tape. Screws attached to a metal plate were then inserted through the holes bored in the PDMS (the tape was closer to the plate) (Figure 6B). A second metal plate was aligned on the screws, and wing nuts were used to clamp the piece of PDMS to the channel system. The small piece of PDMS served as both a surface for adsorption of protein and as a gasket to seal the device.

We used this structure to perform a simple immunoassay similar to that described by Bernard et al. (Figure 7).⁹ Mouse IgG was introduced into every other channel. Bovine serum

albumin (BSA, 1%) was introduced in the remaining channels. After 1 h, the channel system was rinsed using a 12-channel pipettor to deliver 50 μL of fluid to each input reservoir. After rinsing, the small piece of PDMS was removed, rotated 90°, and clamped to the channel system again. The newly exposed surfaces of the piece of PDMS were blocked with BSA, added via the pipettor, to prevent nonspecific adsorption of the target molecule. Anti-mouse IgG antibodies conjugated to fluorophores were introduced into selected channels to create a pattern of squares, which were detected using two-color scanning fluorescent microscopy (Figure 7C).

3-D Fluidic Channels. Many applications of microfluidic devices would benefit from 3-D channel systems.^{19,37,38} Fabrication of channels in 3D allows for compact channel systems, spiral channels, channels that cross over one another without mixing, and certain useful phenomena that may be difficult to obtain with 2-D systems, e.g., mixing by chaotic advection.³⁹ Our laboratory previously developed what we call the “membrane sandwich” method for production of 3-D microfluidic channels using membranes of PDMS.¹⁹ This method uses two masters: one is a multilevel positive relief of photoresist on a silicon wafer, and the other is a layer of PDMS also containing a positive relief structure. Using the silicon and PDMS masters, we can obtain a membrane of PDMS containing features on both sides and connections between the features. We used solid-object printing to produce a similar design but did not need to perform multilevel photolithography or to produce masters in two different materials. In addition, alignment is simple because large complementary shapes can be fabricated in each half of the mold to allow mating (Figure 8). The solid-object printer produced two halves of a mold containing raised features. Half (the bottom half, Figure 8A) had a layer of features that were 500 μm tall, 500 μm wide, and 3.5 mm long. Each end of these features had a raised cube (500 μm tall) such that the total height was 1 mm at the ends. The cubes acted to form connections with the features (500 μm tall, 500 μm wide, and 3.5 mm long) on the other half (the top half, Figure 8B) of the mold. The bottom half was surrounded by a wall (1.5 mm tall, 3 mm thick) around the perimeter of the mold. Areas of 3 mm \times 3 mm at the intersections of the walls were left void for alignment with 3 mm \times 3 mm \times 1.5 mm features on the top half of the mold. One of the walls also contained a gap in the middle for access to the interior of the mold. To assemble the mold, its two halves were pressed together to create intimate contact between the features on each half. Once the mold was assembled, PDMS prepolymer could be added via syringe and cured. The mold was reused three times before it broke on handling; we believe, with more careful handling, the mold could be reused 10 or more times. After removal from the mold, the PDMS membrane was sealed on both sides with silicone tape and filled with fluid. Figure 8D shows a “basket weave” pattern that was fabricated using this technique.¹⁹

(37) Jo, B.-H.; Van Lerberghe, L. M.; Motsegood, K. M.; Beebe, D. J. *J. Microelectromech. Syst.* **2000**, *9*, 76–81.

(38) Unger, M. A.; Chou, H.-P.; Thorsen, T.; Scherer, A.; Quake, S. R. *Science* **2000**, *288*, 113–116.

(39) Liu, R. H.; Stremmer, M. A.; Sharp, K. V.; Olsen, M. G.; Santiago, J. G.; Adrian, R. J.; Aref, H.; Beebe, D. J. *J. Microelectromech. Syst.* **2000**, *9*, 190–197.

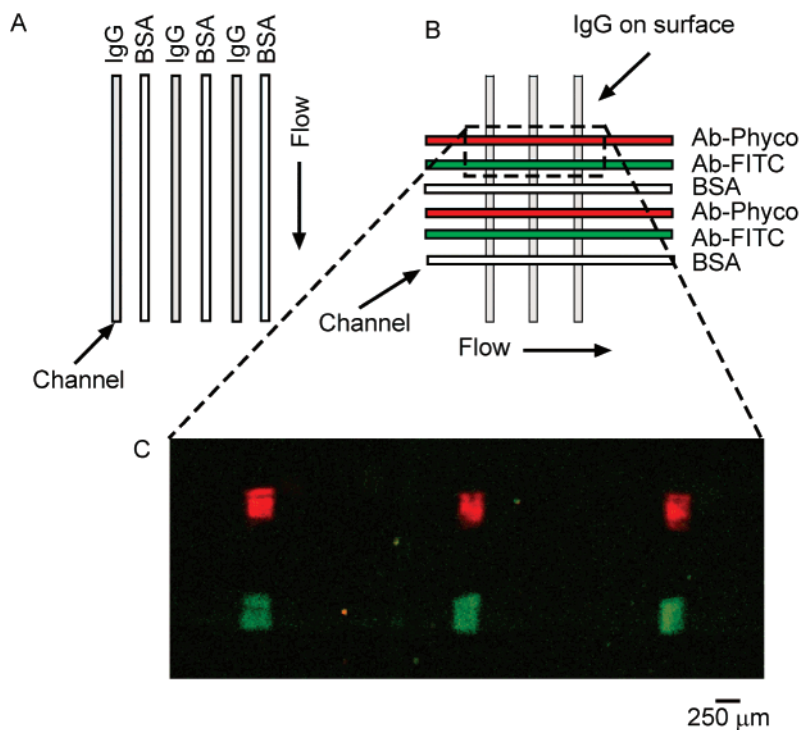


Figure 7. (A) Mouse IgG ($100 \mu\text{g}/\text{mL}$) was placed in every other channel (only 6 of the 12 are shown). A solution of 1% BSA was placed in the remaining channels. The channels were initially filled using suction, and the solutions then flowed ($\sim 25 \mu\text{L}/\text{h}$) under hydrodynamic pressure. After 1 h, the channels were rinsed and the patterned piece of PDMS was removed, rotated 90° , and clamped to the surface again. Buffer containing BSA was then placed in the channels for 30 min to block the newly exposed surface from nonspecific adsorption. (B) Solutions of goat anti-mouse IgG conjugated to phycoerythrin (Ab-phyco, $5 \mu\text{g}/\text{mL}$) and fluorescein (Ab-FITC, $20 \mu\text{g}/\text{mL}$) were placed in adjacent channels. The remaining channels were filled with 1% BSA. After 1 h, the channel system was rinsed and removed from the piece of PDMS. (C) The squares patterned at the intersection of mouse IgG and Ab-Phyco (red) and Ab-FITC (green) (area indicated by dashed box in B) were visualized using scanning fluorescent microscopy. The micrograph is a composite image of the two fluorophores taken with different filter sets. False color was added, and the intensities of the two colors were normalized to each other using Photoshop.

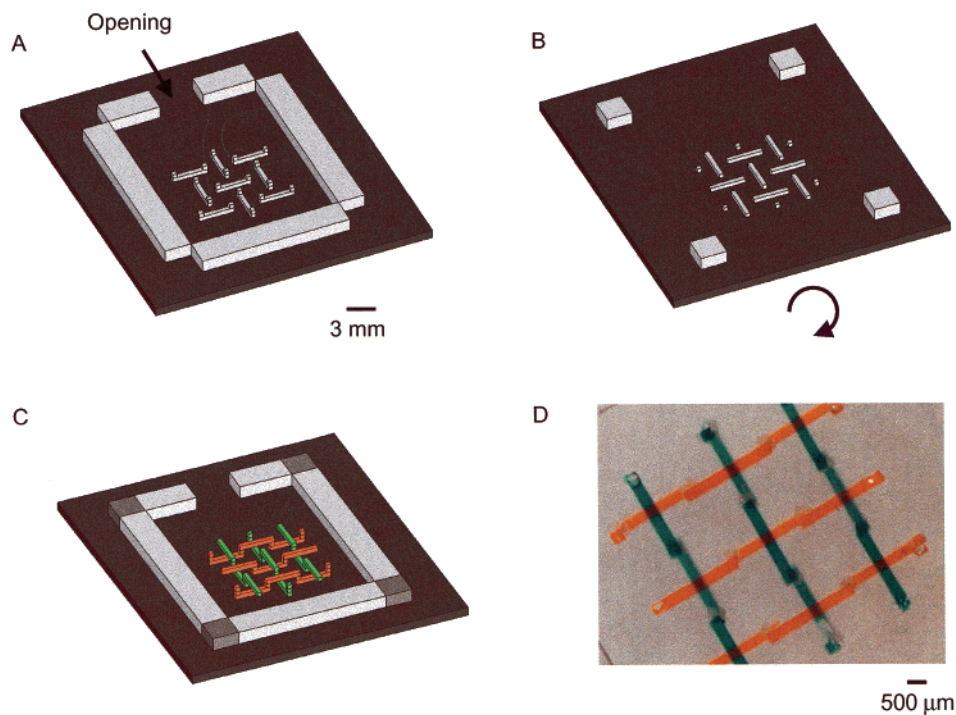


Figure 8. Scheme for fabrication of a mold for a basket weave pattern for crossing, nonintersecting channels. The pattern comprises three layers of features. Two layers are present in (A), and one layer is present in (B). (C) To assemble the mold, (B) is rotated 180° (arrow in B) and brought into contact with (A). The four squares on (B) fit into complementary shapes on (A). When (A) and (B) are brought into contact by pressure, the features on both halves align to form a basket weave pattern (top surface omitted for clarity). PDMS prepolymer is injected through an opening in the wall of the mold. After curing for 1 h, the halves are separated, and the PDMS replica is removed. (D) The PDMS was oxidized by exposure to an air plasma and sealed on both sides with silicone tape. The channels were filled with red and green ink.

CONCLUSIONS

We have developed a method for prototyping microfluidic systems in PDMS using solid-object printing. This method has several advantages over photolithography: (i) Fabrication is simple; the process does not require spin coating, alignment of masks, timed exposures to light or development solutions, or access to a cleanroom. (ii) Solid-object printing can produce structures with dimensions larger than a 3-in. Si wafer—including height up to 8 in.; the technique spans dimensions from the submillimeter to the centimeter scale. (iii) The method is fast (~2 h to fabricate the devices discussed here) and not labor intensive. (iv) The thermoplastic build material can be used either as a master or in a sacrificial mold. (v) The build material is nontoxic, and the printer can be used in an office environment without ventilation.

The method also has disadvantages: (i) The resolution of the technique is lower (250- μm channels are the minimum that can be fabricated reliably) than photolithography. (ii) The build material is soft and can be deformed or scratched, especially at elevated temperatures. (iii) The surface roughness limits the optical performance of structures. (iv) The method requires access to a solid-object printer (although many commercial prototyping firms will provide objects in less than 1 week).

Even with these limitations, we believe this method will find use in the prototyping of microfluidic devices that need multilevel features or to integrate macroscopic equipment. In addition, the method is especially appropriate for laboratories that want to fabricate devices but do not have the facilities for, or experience with, photolithography.

EXPERIMENTAL SECTION

Fabrication. Designs for masters were drawn in 3-D in Form.Z (version 3.5, auto.des.sys, Columbus, OH, <http://www.formz.com>) and exported as stereolithography files (.stl format). The files were then printed in Thermojet 2000 build material on a Thermojet (3D Systems, Valencia, CA, <http://www.3dsystems.com>) solid-object printer. Several small masters could be printed at once. We used a putty knife heated in a Bunsen burner to separate the masters from one another. Degassed, liquid PDMS prepolymer (10:1 base: curing agent, Sylgard 184, Dow Corning, Midland, MI) was then poured over the master. Some masters had 6-mm-tall and 3-mm-wide walls around the perimeter to contain the PDMS. For masters without walls, we made walls by taping 1-in.-wide silicone tape (Ideal Tape, Lowell, MA, <http://www.idealtape.com>) around the perimeter of the master. The PDMS was cured at 70 °C for 1–2 h. After removal from the oven and cooling to room temperature, the cured PDMS replica was peeled carefully from the master.

To seal a PDMS replica irreversibly, the replica and a glass slide or flat piece of PDMS were oxidized for 1 min at 100 W in a plasma cleaner (PDC-32G, Harrick, PA, <http://www.harricksci.com>) in ambient air at 1.5–2 Torr. Bringing the two oxidized surfaces into conformal contact within ~1 min after removal from the plasma cleaner allowed a strong bond to form. The oxidation process could also be used to render the PDMS channels hydrophilic.

For annealed masters, a negative relief of a channel system was printed. This inverse master was then placed on top of a transparency (plain paper copier, 3M, Austin, TX) that was on a hot plate. After ~5 min at 95 °C, the master melted into contact

with the transparency. The master and transparency were cooled at –20 °C until the transparency detached from the master. PDMS was molded against the annealed inverse master to produce another master. The PDMS master contained the channel system in positive relief. The PDMS master was oxidized for 1 min. The oxidized master was placed in a vacuum desiccator with a vial containing a few drops of tridecafluoro-1,1,2,2-tetrahydrooctyl-1-trichlorosilane (United Chemical Technologies, Bristol, PA, <http://www.unitedchem.com>) for 2 h at reduced pressure. PDMS replicas containing embedded channels could then be fabricated by molding against the silanized PDMS master.

Epoxy replicas of some masters were produced since epoxy is more durable than the thermoplastic material. Epoxy replicas were also produced for profilometry measurements. A UV-curable epoxy (UVO 114, Epoxy Technology, Billerica, MA, <http://www.epotek.com>) was poured over a PDMS replica. The epoxy was cured by exposure to UV light from a 100-W mercury lamp for 1–3 h, depending on the thickness of the epoxy. The PDMS replica could be easily peeled from the epoxy. Surface characterization of the PDMS was carried out by profilometry (Alpha-Step 200, Tencor, <http://www.tencor.com>) on epoxy replicas and by SEM (JSM-6400, JEOL, Peabody, MA, <http://www.jeol.com>) on gold-coated PDMS.

Applications. (1) 3-D Cross. When the PDMS was removed from the master, the vertical pillar broke and detached from the master. The PDMS with the embedded pillar was then heated using a heat gun to melt the build material. The material was removed using suction. For Figure 1, the device was conformally sealed to PDMS. For Figure 3, the device was oxidized for 1 min and then sealed with silicone tape. An optical fiber (P50-2 UV, core diameter 50 μm , cladding thickness 125 μm , Ocean Optics) with the coating removed was conformally sealed in the vertical channel. A solution of fluorescein in phosphate-buffered saline was introduced into the channels by capillary action. Fluorescent micrographs were obtained using an inverted microscope.

(2) Microfluidic Mixer. After removal from the master, holes were cut in the reservoirs with a 1-mm circular punch. PDMS replicas were oxidized for 1 min and sealed with silicone tape (1 in. wide, Ideal). Syringes (1 mL, Henke-Sass, Wolf) were connected to the device by polyethylene tubing (i.d. 0.38 mm, o.d. 1.09 mm, Becton Dickinson) that was pressure fit over a 27-gauge needle (Becton Dickinson) and into a 1-mm reservoir in the device. Solutions of 20% water–80% glycerol with and without purple ink (Waterman) were pumped into the device at a rate of 15 mL/h by a syringe pump (Harvard Apparatus). Results were visualized using a digital camera. The intensity profiles were determined using Scion Image (Scion Corp., <http://www.scioncorp.com>).

(3) Interface between a Pipettor and Microfluidic Channels. A PDMS replica was sealed to two pieces of silicone tape (2 in. wide, Ideal). The tape covered the entire device except for an ~1-cm region where the 12 channels are parallel (see Figure 6A). Four holes were bored into the PDMS and silicone tape. A small piece of PDMS (~1 \times 1 cm², ~1 mm thick) was placed in contact with the exposed region of the PDMS replica. The replica and piece of PDMS were placed between two metal plates connected by four screws. Wing nuts were used to provide pressure to clamp the piece of PDMS to the channel system to form a watertight seal. Solutions of mouse IgG (100 $\mu\text{g}/\text{mL}$ in 50

mM Na₂CO₃, pH 9.6) and BSA (1% in 50 mM Tris, 150 mM NaCl, pH 8) were allowed to flow through six channels each (alternating laterally) under hydrodynamic pressure for 1 h. The replica was rinsed (50 mM Tris, 100 mM NaCl, 0.05% Tween 20, pH 8), removed, rotated 90°, and clamped to the piece of PDMS again. BSA was allowed to flow through six channels for 30 min to block the surface from nonspecific adsorption of antibodies. Solutions of goat anti-mouse IgG conjugated to FITC (20 μg/mL in 1% BSA, 50 mM Tris, 150 mM NaCl, pH 8, Rockland) or phycoerythrin (5 μg/mL in 1% BSA, 50 mM Tris, 150 mM NaCl, pH 8, Rockland) and BSA flowed through the device in designated channels for 1 h. The channels were then rinsed, the replica was removed from the patterned piece of PDMS, and the PDMS was dried. The results of the assay were visualized using two-color detection on a scanning fluorescent microscope (Leica).

(4) 3-D Channels. Two halves of a mold were fitted together by applying pressure using a small vice. Liquid PDMS was injected

via syringe into the mold through an opening in one wall bounding the mold. After curing for 1 h, the replica was removed from the mold. The replica was oxidized for 1 min and sealed with silicone tape. Solutions of red and green ink (Waterman) were injected into the channels, which filled by capillary action.

ACKNOWLEDGMENT

We thank Kimo Griggs and Judith Hodge (Harvard University Graduate School of Design) for assistance with the solid-object printer. We also thank Kateri Paul for obtaining the SEM images. This work was supported by DARPA and the National Science Foundation (Grants ECS-9729405 and ECS-0004030).

Received for review August 21, 2001. Accepted January 16, 2002.

AC010938Q